Research Article

Received: 18 September 2019 Revised: 29 February 2020 Accepted article published: 2 April 2020 Published online in Wiley Online Library: 18 April 2020

(wileyonlinelibrary.com) DOI 10.1002/jsfa.10400

Nano-vesicular formulation of propolis and cytotoxic effects in a 3D spheroid model of lung cancer

Esra Ilhan-Ayisigi,[a,b†] Fulden Ulucan,[c†] Ecem Saygili,[a] Pelin Saglam-Metiner,[a] Sultan Gulce-Iz[a,c,d] and Ozlem Yesil-Celiktas[a,c*]

Abstract

BACKGROUND: Propolis exhibits therapeutic properties due to the presence of phenolic acids, esters, and flavonoids. The scope of this study was to develop a nano-vesicular formulation and establish a three-dimensional (3D) spheroid model in which lung cancer is recapitulated.

RESULTS: Niosome vesicles doped with galangin-rich propolis extract were synthesized by the ether injection method using a cholesterol : surfactant mass ratio of 1 : 3 at 40 °C for 1 h. Formulated niosomes were administered to 3D lung cancer spheroid model and the cytotoxicity was compared with that of a two-dimensional (2D) setting. The galangin content was determined as 86 μg mg^{-1} propolis extract by ultra-performance liquid chromatography (UPLC). The particle size of loaded niosome was 151 ± 2.84 nm with a polydispersity index (PDI) of about 0.232, and an encapsulation efficiency of 70% was achieved.

CONCLUSION: The decrease in cell viability and the scattering in the 3D spheroids of A549 lung cancer cells treated with propolis-loaded niosomes were notable, indicating a profound cytotoxic effect and suggesting that they can be utilized as an effective nano-vesicle.

Keywords: niosome; propolis; galangin; 3D cell culture; lung cancer

INTRODUCTION

Niosomes and liposomes are genuinely novel drug-delivery systems, which are known as vesicular delivery systems. Due to their non-toxic nature and their ability to encapsulate many hydrophilic and lipophilic compounds, these vesicles have been investigated in the pharmaceutical industry. However, niosomes have advantages over liposomes due to better chemical stability and comparatively low production costs.[1,2] Moreover, niosomes consist of a nonionic surfactant, cholesterol and diethyl ether; they therefore possess a structure consisting of hydrophilic, amphiphilic, and lipophilic parts together.[3] With these features, niosomes are capable of encapsulating natural therapeutic agents and pharmaceuticals such as curcumin, candesartan cilexetil, and enoxacin, improving the oral bioavailability of poorly absorbed drugs and enhancing skin penetration of various drug molecules.[4] Propolis is a natural therapeutic agent; it is a brownish, waxy product collected from various plant sources by honeybees and it contains fatty acids, terpenes, β-steroids, aromatic aldehydes, and alcohols, along with active compounds such as phenolic acid esters and flavonoids.[5] Propolis is reported to possess a broad spectrum of biological activity, such as anticancer, antioxidant, antiviral, anti-parasitic, anti-inflammatory, antibiotic, antifungal, anti-ulcer, and anti-hepatotoxic activity.[6,7] Its antimicrobial properties are mainly attributed to the flavonone pinocembrin, to the flavonol galangin, and to a caffeic acid derivative, with a mechanism of action probably based on the inhibition of bacterial RNA-polymerase.[8] However, it is not directly related to the concentration of biological active substances, but it depends on synergistic activity between various active ingredients.[9] The recorded use of propolis dates back to 300 BC due to its therapeutic effects.[10] The limited human studies on propolis bioavailability have shown that propolis exhibits low bioavailability, which in turn reduces the therapeutic effects. Moreover, studies showed that one of the main phenolic acids (artepillin C) in

* *Correspondence to: O Yesil-Celiktas, Department of Bioengineering, Faculty of Engineering, Ege University, 35100 Bornova, Izmir, Turkey, E-mail: ozlem.yesil.celiktas@ege.edu.tr*

† *E.I.-A. and F.U. contributed equally as first authors.*

a *Department of Bioengineering, Faculty of Engineering, Ege University, Bornova, Turkey*

b *Genetic and Bioengineering Department, Faculty of Engineering and Architecture, Ahi Evran University, Kirsehir, Turkey*

c *Biomedical Technologies Graduate Programme, Graduate School of Natural and Applied Sciences, Ege University, Bornova, Turkey*

d *Department of Biomedical Engineering, Eindhoven University of Technology, Eindhoven, The Netherlands*

propolis is absorbed less efficiently than *p*-coumaric acid and its intestinal absorption was lower than its *in vitro* transcellular passive diffusion.[11] Because of the low bioavailability and hydrophobicity of propolis, preparation and characterization of niosomes loaded with propolis extracts are needed for higher therapeutic efficiency.[12] Once a drug carrier system is designed and formulated, novel strategies are required to evaluate the efficacy as 2D cell culture has many limitations such as lack of interactions between the cellular and extracellular matrix, changes in polarity and cell morphology, inability to mimic *in vivo* pathophysiology, biomechano-chemical structure, complex function of tissue organization, and tissue microenvironment.[13] Disease models generated with 3D spheroid cultures can recapitulate specific disease states and fulfill this requirement. Various techniques are employed for the preparation of 3D spheroid cultures such as spinner flask, hanging drop, scaffolds, matrigel cultures, non-adhesive molds, and the liquid overlay method.[14,15] Homogenous shape, volume, and viability are important parameters, which may vary based on the method. Pre-selection of spheroids is therefore recommended to obtain reliable and reproducible data in cytotoxicity tests. The objective of the present study was to identify the major compound in propolis extract and assess dose-dependent cytotoxic effects of both propolis extract and a commercial propolis on A549 lung cancer and BEAS-2B healthy lung cells, incorporate galangin rich propolis in niosomes, and finally investigate the effects in a 3D spheroid culture modeling lung cancer.

MATERIALS AND METHODS

Materials and reagents

Propolis was obtained from Yildizeli, Sivas, Turkey. Folin–Ciocalteu's phenol reagent, silica gel F254 20 × 20 cm plaques, HP silica gel F254 20 × 20 cm plaques, NP-PEG reagents, poliamide, RP silica gel C18, ethanol, dichloromethane (DCM), methanol, sulfuric acid, dimethylsulfoxide DMSO-d6, Tween 80, and diethyl ether were purchased from Merck (Darmstadt, Germany). Cholesterol, high-performance liquid chromatography (HPLC)-grade ethanol, acetonitrile, methanol, and tetrahidrofurane were from Sigma-Aldrich (Munich, Germany). Sodium carbonate was supplied by AppliChem GmbH (Darmstadt, Germany). Ultrapure water was provided from an ultrapure water system (Sartorius Arium 611, Sartorius-Stedim, Gottingen, Germany).

Propolis extraction

Ultrasonic-assisted successive extraction was used to extract 50 mg of propolis with 20 mL ethanol for 30 min at 40 °C.[16] The collected supernatant was evaporated with SpeedVac concentrator (SC250EXP Thermo Fisher Scientific Inc., MA, USA) and kept in the freezer (−20 °C) until further use.

Characterization of propolis extract

Isolation of the major flavonoid compound in propolis extract was carried out using a series of analytical methods. After isolation of the desired bands with preparative thin-layer chromatography (TLC), constituents were partitioned with column chromatography and then validated by nuclear magnetic resonance (^{1}H-NMR) and liquid chromatography electrospray ionization mass spectroscopy (LC-ESI-MS).

Preparative thin layer and column chromatography

Propolis extract was pipetted on the prep-TLC silica plates by line application. The solvent system was selected as 95 : 5 DCM:methanol. After ultraviolet (UV) imaging, a UV active substance at 366 nm was cut off from the TLC plate as a line and dissolved in methanol. Thin-layer chromatography was repeated to control the transfer of the substance into methanol. A partition technique based on polarity was used for isolation. Thus, an amount of reverse-phase C18 silica gel was conditioned with the mobile phase ranging from 50% to 70% methanol. Fractions were collected in the test tubes and TLC and UV imaging were applied to track composition. The isolated compound was confirmed with the ^{1}H-NMR and LC-ESI-MS techniques.

H-NMR and LC-ESI-MS analysis for validation of the major compound

The major flavonoid compound, galangin, isolated from propolis extract, was confirmed by both the ^{1}H-NMR and LC-ESI-MS techniques. The isolate was lyophilized and characterized at 400 MHz by Varian Mercury 400 Plus NMR (Varian Inc., CA, USA) with DMSO-d6. Then the molecular mass was determined by the LC-ESI-MS (Thermo Quantum Access Max, Thermo Fisher Scientific Inc.) technique with positive and negative modes between the sizes of 100–1000 Da.

Formulation and characterization of niosomes

The ether injection method was applied to synthesize niosomes. Cholesterol and Tween 80 were dissolved in diethyl ether at a mass ratio of 1 : 3. A certain amount of propolis extract was added to the mixture along with 10 mL 0.01 mol L^{-1} phosphate buffer solution (Sigma-Aldrich, Poole, UK) (PBS) (pH 7.4) buffer and sonicated for 1 h at 40 °C.[17] Subsequently, synthesized niosomes were centrifuged (MiniSpin, Eppendorf AG, Hamburg, Germany) at 12100 *g* for 20 min and supernatant was separated from the pellet. Then the pellet was washed with ultra-pure water twice and lyophilized after being frozen at −86 °C. The experiments were carried out in duplicates.

Encapsulation efficiency by ultra-performance liquid chromatography-diode array detector (UPLC-DAD)

After niosome synthesis, the mixture was centrifugated and the supernatant was quantified by UPLC-DAD to determine the unloaded galangin amount. An ACE 5 C18 (4.6 × 250 mm) column (Advanced Chromatography Technologies Ltd., Aberdeen, Scotland) was used for the analysis and the mobile phase consisted of 1% tetrahidrofurane (pH 3.0 with H_3PO_4) and acetonitrile.[18] Encapsulation efficiency (EE%) was determined based on the galangin content of extract by the ratio of actual and theoretical propolis extract loaded (Eqn 1):

$$EE\% = \frac{\text{amount of propolis extract entrapped}}{\text{total amount of propolis extract used}} \times 100 \quad (1)$$

Particle size analysis

Size distributions and zeta potential values were measured with a Malvern Zetasizer Nano-ZS (Malvern Instruments Ltd, Worcestershire, UK) after the synthesized niosome suspensions were diluted fourfold in Milli-Q water. The results were determined by the average of three cycles of many scans (autocalculated by device) and the average size was presented as mean value ± standard error of the mean.

Differential scanning calorimeter (DSC) analysis

The thermal properties of the vesicles were analyzed by differential scanning calorimetry (DSC, DSC 8000 model, PerkinElmer, Inc., MA, USA). About 5 mg of lyophilized samples was compressed and loaded in standard aluminium pans, and samples were purged with pure dry nitrogen at a flow rate of 5 mL min^{-1}. The analysis was carried out at a temperature range of 20–200 °C with an increase rate of 10 °C min^{-1}.

Fourier transform infrared spectroscopy (FTIR) analysis

Fourier transform infrared spectroscopy spectra of propolis extract, propolis-loaded niosome vesicles, cholesterol, and Tween 80 surfactant, as individual components in the formulation, were recorded between wave lengths of 650–4000 cm^{-1} on a Perkin-Elmer Spectrum 100 instrument.

Scanning electron microscopy (SEM) analysis

To investigate the morphology of the niosome particles, lyophilized niosome samples were placed onto metal grids with the help of double-sided adhesive tape and coated with gold by using Emitech K550X sputter coater.

Cytotoxicity in 2D and 3D spheroids

Maintenance of the cell lines

A BEAS-2B (human bronchial epithelium) non-tumor cell line and A549 human epithelial lung adenocarcinoma cell lines were obtained from American Cell Culture Collection (ATCC, Mannassas, VA, USA). Cells were maintained in a Dulbecco's Modified Eagle Medium (DMEM) supplemented with 10% fetal calf serum, 1% L-glutamine, 0.1% 10 mg mL^{-1} gentamicin. All cell culture reagents were supplied by Sigma-Aldrich.

Cytotoxicity of free propolis in 2D cell culture

An initial concentration of 1×10^4 cells / well were seeded on 96 well plates and incubated overnight at 37 °C, 5% CO_2 prior to propolis extract treatment to reach 90% confluence. For comparison, a commercial propolis extract (BEEO™, Istanbul Technical University-Advanced Research and Innovation center (ITU-ARI) Teknokent, Istanbul, Turkey) was tested as well. Ethanol at a concentration of ≤0.1% v/v, not causing any toxicity to cells, was used as a control. Untreated cells were used as a negative control (cells were treated with growth medium only), and dimethylsulfoxide (DMSO) (100% v/v) was used as a positive control. Cells were treated with different concentrations of propolis extract, ranging from 400 μg mL^{-1} to 0.78125 μg mL^{-1} with four replicates, and were incubated with 37 °C, 5% CO_2 at 72 h. At the end of the treatment time, the medium was removed and 10% MTT (3-(4,5-dimethyl-2-thiazolyl)-2,5-diphenyl-2H-tetrazoliumbromide)) solution was added to each well at 100 μL. This was diluted in fresh cell-culture medium from 5 mg mL^{-1} MTT stock solution and incubated for 3 h at 37 °C in a dark environment. After the medium was removed and DMSO was added to each well at 100 μL, the absorbance was measured by a microplate reader at 570 nm (SpectraMax 190, Molecular Devices, Sunnyvale, CA, USA). The cell viabilities and IC_{50} values were determined by using GraphPad Prism 5.0.[7]

Cytotoxicity of propolis-loaded niosomes in 2D and 3D spheroids

For the 2D cytotoxicity assay, A549 and BEAS-2B cells were seeded in a 96-well plate at 1×10^3 cells / well and incubated overnight at 37 °C, 5% CO_2. After substance applications for 7 days, an MTT assay was performed. Untreated cells were used as a negative control, and DMSO as a positive control. On days 3 and 5, the medium (including substance treatment) of the cells was changed. Then, the cell viabilities of propolis-loaded niosomes, the equivalent amount of propolis, and empty niosomes were determined by using GraphPad Prism 5.0. Propolis was applied at a concentration of about four times higher than the IC_{50} value of free propolis on A549 cells (100 μg mL^{-1}). Various studies have indicated that the bulk drug may be loaded into carrier systems in excess of three times to increase its long-term efficacy and bioavailability, and to reduce degradation in *in vitro* / *in vivo* studies.[19]

For the 3D cytotoxicity test, the formation of 3D spheroid structures of A549 and BEAS-2B cells was first achieved using a 3D Petri Dish® micro-tissue mold (size S, 8 × 12 array, 400 μm × D 800 μm diameters) (Micro Tissues Inc., Providence, RI, USA). Sterile agar solution was transferred into the chamber of the mold. After gelation occurred, the mold was inverted with the aid of a forceps and placed in a well plate. Then cells were seeded into conditioned 3D micro tissue mold at 1×10^5 cells/mold for the formation of spheroids, and incubated at 37 °C, 5% CO_2. Spheroid structures were observed daily under an inverted light microscope (Zeiss, AX10, Oberkochen, Germany) for 10 days and diameters were measured by the ImageJ program. After niosome treatment for 7 days, the live/dead assay (Molecular Probes, Invitrogen, Thermo Fisher Scientific) was performed to screen the cytotoxicity of the propolis-loaded niosomes and empty niosomes on both cancer and healthy cell spheroids by inverted fluorescent microscope (Zeiss).[20] Then, spheroid sizes and live/dead cell numbers were measured by the ImageJ program. For the live/dead assay, after removing the medium on the cell spheroids, 2 μ mol L^{-1} calcein AM and 4 μ mol L^{-1} EthD-1 (ethidium homodimer-1) solution containing PBS was added directly to spheroids and incubated for 30 min at room temperature. Then excess dye was washed with PBS and samples were imaged by inverted fluorescent microscope. The polyanionic dye calcein AM is well retained within live cells, producing an intense uniform green fluorescence, where fluorometric observation is made at ex/em ~495 nm/~515 nm wavelength. EthD-1 enters cells with damaged membranes and binds to nucleic acids, producing a bright red fluorescence in dead cells, and fluorometric observation is made at ex/em ~495/~635 nm wavelength (Invitrogen™ L3224).

Statistical analysis

The results were analyzed using a GraphPad Prism 5.0 program. Two-item experiments involving multiple groups were evaluated by two-way ANOVA, with a Bonferroni post-test and a confidence interval of ±95% ($P < 0.05$). Spheroid sizes and live / dead cell numbers were measured with an ImageJ program.

RESULTS

Characterization of propolis extract

As propolis extract is extremely rich in phenolic acids and flavonoids, determination and quantification of the major compounds was imperative prior to encapsulation in the niosome formulation. Thin-layer chromatography and column chromatography methods were applied, followed by ^{1}H-NMR (Fig. 1(A), (B)) and LC-ESI-MS analyses (Fig. 1(C)). In Fig. 1(A), the 0–8 ppm region represents terpenes,[21] sugars, and phenolics, and the 6–8.1 ppm region specifically refers to phenolic compounds in Fig. 1(B). ^{1}H-NMR (400 MHz, DMSO-d6) shifts δ: 8.02 (2H, d, J = 7.5 Hz, H-2′, 6′), 7.56 (3H, m, H-3′, 4′, 5′), 6.36 (1H, br.s, H-8), 6.07 (1H, br.s, H-6) indicated the presence of a flavonoid in Fig. 1(A) and (B). In Fig. 1(C), the LC-ESI- MS results

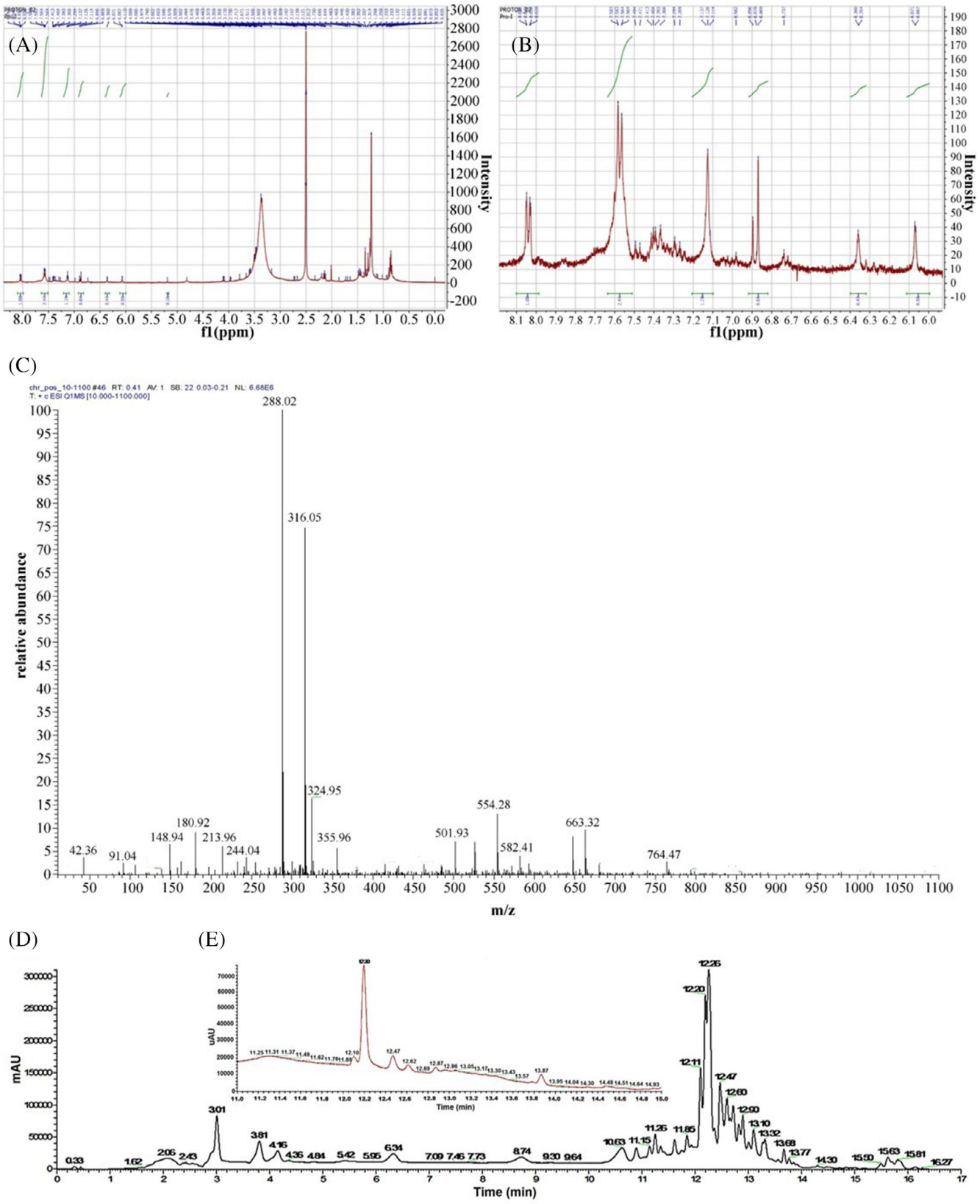

Figure 1. Nuclear magnetic resonance spectra of the major compound in the 0–8 ppm region (A); 6–8.1 ppm region (B); the LC-ESI-MS result depicting the molecular weight of the major compound as 288.02 g mol^{-1} in positive mode (C); UPLC-DAD chromatograms of galangin in propolis extract (D) and galangin (E).

showed that molecular weight of the main compound was 288.02 g mol^{-1} in positive mode. However, using ammonium resulted in a slight decrease in the molecular weight to 270.24 g mol^{-1}. According to the results of ^{1}H-NMR and LC-ESI-MS positive mode analyses, the major compound was identified as galangin. The UPLC-DAD method was used to quantify the amount of galangin in the propolis extract (Fig. 1(D), (E)). The retention time was 12.18 min, which is consistent with the results of Verza *et al.*[18] Consequently, the amount of galangin in propolis extract was measured as 86 µg galangin per mg propolis extract.

Synthesis and characterization of niosome vesicles

Niosome vesicles were synthesized using the ether injection method, where Tween 80 and cholesterol were used to build the lamellar structure. Particle-size distributions of both empty and loaded niosomes exhibited a comparatively narrow distribution represented by single peaks facilitating a uniform drug release (Fig. 2(A), (B)). The particle size of empty niosomes was 141.2 ± 4.54 nm with a polydispersity index (PDI) value of 0.21, and loaded particles exerted a similar particle size of 151 ± 2.84 nm with a PDI value of 0.23. The zeta potentials of −18.6 ± 0.59 mV and − 30.9 ± 0.33 mV were measured for empty and propolis-loaded niosomes, respectively. As for drug entrapment, galangin-rich propolis extract was loaded with an encapsulation efficiency of 70%.

Differential scanning calorimeter studies were performed to investigate the physical states and intermolecular interactions of propolis extract and niosome vesicles. Propolis-free vesicles showed endothermic peaks between 39.96–48.44 °C and 113.23–137.25 °C, and the endothermic peaks of loaded vesicles were between 38.14–64.19 °C and at 116.75 °C. A degradation line was observed over 150 °C due to thermal degradation of propolis extract (Fig. 2(C)). Thermal peaks achieved for propolis extract were at the same range as described in a previous study.[12] As the characteristic endothermic peak of propolis extract at 93.47 °C cannot be observed in loaded niosomes, it can be concluded that the active substance is in amorphous form in niosome vesicles. Fourier transform infrared spectroscopy spectra of propolis extract, loaded niosomes, cholesterol, and Tween 80 as individual components in the formulation are depicted in Fig. 2(D). The FTIR spectrum of the propolis extract showed a typical hydrogen-bonded O—H stretch of phenolic compounds at 3286.82 cm^{-1} (phenolic hydroxyl group) and bands at 2918.74 and 2849.79 cm^{-1} could be attributed to ethanol.[22] Absorptions at 1686.75, 1631.77, 1602.53, 1512.59, and 1449.61 cm^{-1} corresponded to the C=C, C=O and CH vibrations of aromatic ring.[12] Although the band at 1370.64 cm^{-1} was not identified, it is thought that the band at 1260.48 cm^{-1} would be related to the vibration of C—O group of polyols, such as hydroxyflavonoids. The band at 1159.37 cm^{-1} was considered to occur due to lipids and alcohol groups (stretching of C—O and bending of C–OH), the band at 1114.55 cm^{-1} could be related to tertiary alcohols, and the band at 1086.55 cm^{-1} related to the C—O stretching and –OH deformation of secondary alcohols. The band at 1033.57 cm^{-1} was probably related to primary and secondary alcohols and to C—O— stretching of the ester group.[22] All other bands of propolis extract at 978.62, 877.69, 832.60, 811.60, 766.58, 740.60, and 697.53 cm^{-1}, were related to angular deformation outside the plane of aromatic C—H and alkenes.[12] Cholesterol showed peaks of the hydroxyl

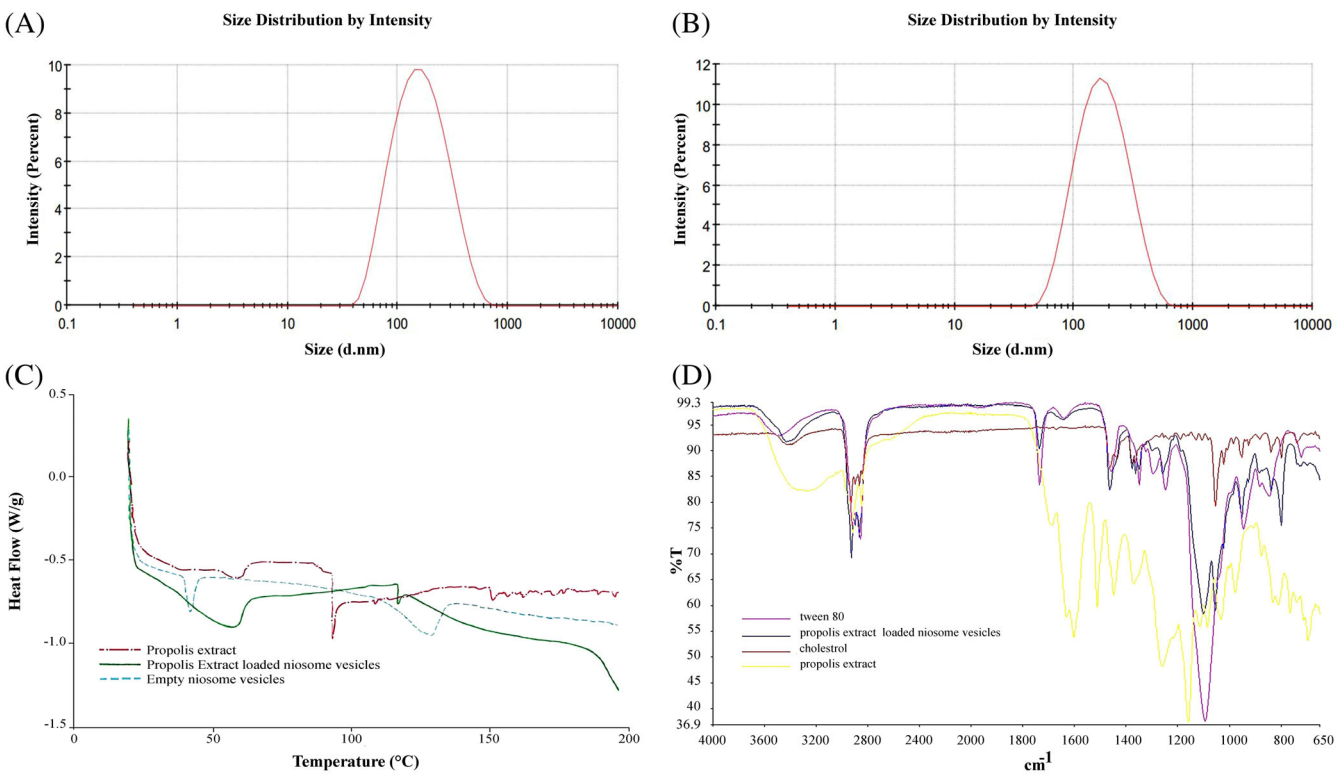

Figure 2. Dynamic light-scattering results for unloaded (A) and propolis-loaded niosome vesicles (B); DSC analysis of propolis extract, empty niosome particles and niosome particles loaded with propolis extract (C) and FTIR spectra of propolis extract, propolis extract-loaded niosome vesicles and, cholesterol and Tween 80 as individual components (D).

group[23] at 3413.91 cm^{-1}, and strong aromatic stretching of CH═CH at 2930.80, 2999.83, and 2866.83 cm^{-1}, whereas Tween 80 exhibited a broad and strong band at 3490.92 cm^{-1}, representing the stretching vibrations of O—H. The C═O stretching vibrations appear at 1735.83 cm^{-1} whereas the band at 1095.37 cm^{-1} is assigned to asymmetric C—O stretching vibrations.[24] Similar peaks were obtained from FTIR scans of niosomal formulation, cholesterol, and Tween 80. Results confirmed that the propolis extract had not interacted chemically with any of the ingredients of the niosomal formulation and it was entrapped physically. Scanning electron microscopy micrographs of the outer topographies of empty and loaded niosomes are presented in Fig. 3. Empty niosomes exhibited spherical structures as well as loaded vesicles. However, loaded niosomes were observed to be slightly distorted possibly due to extract loading.

Dose-dependent cytotoxicity of free propolis in 2D cell culture

Cytotoxic effects of propolis extract and commercial propolis were tested dose dependently (400–0.78125 μg mL^{-1}) on A549 lung cancer and BEAS-2B healthy lung cells after 72 h exposure. The results showed that propolis extract exerted a higher cytotoxic effect on cancerous cells in comparison with the healthy cells (Fig. 4). The IC_{50} values of propolis extract were determined as 25.44 ± 4.97 and 55.68 ± 6.24 μg mL^{-1} for A549 lung cancer and BEAS-2B healthy lung cells ($P < 0.05$), whereas 30.65 ± 7.43 μg mL^{-1} and 59.11 ± 7.54 μg mL^{-1} for commercial propolis, respectively ($P < 0.05$).

Cytotoxicity of propolis-loaded niosomes in 2D and 3D spheroids

In this study, the cytotoxicity of propolis-loaded niosomes was investigated both by 2D and 3D cell-culture settings. Cell culture results in 2D setting have been presented by two different approaches. In the first approach, the absorbances of negative control (untreated control cells) at each time slot were considered as 100% of growth and used for cell viability (%) calculations of A549 cells at respective time slots (Fig. 5(A), (C)). Secondly, the absorbance of negative control at 24th hour measurement was considered as 100% of growth and proportioned to the viability values of BEAS-2B cells at respective time slots (Fig. 5(B), (D)). Similar trends were observed in regard to the cytotoxic effects of propolis-loaded niosomes and free propolis, which decreased the cell viability to a level below 50% after 24 h of treatment, whereas empty niosomes proved to be non-cytotoxic because

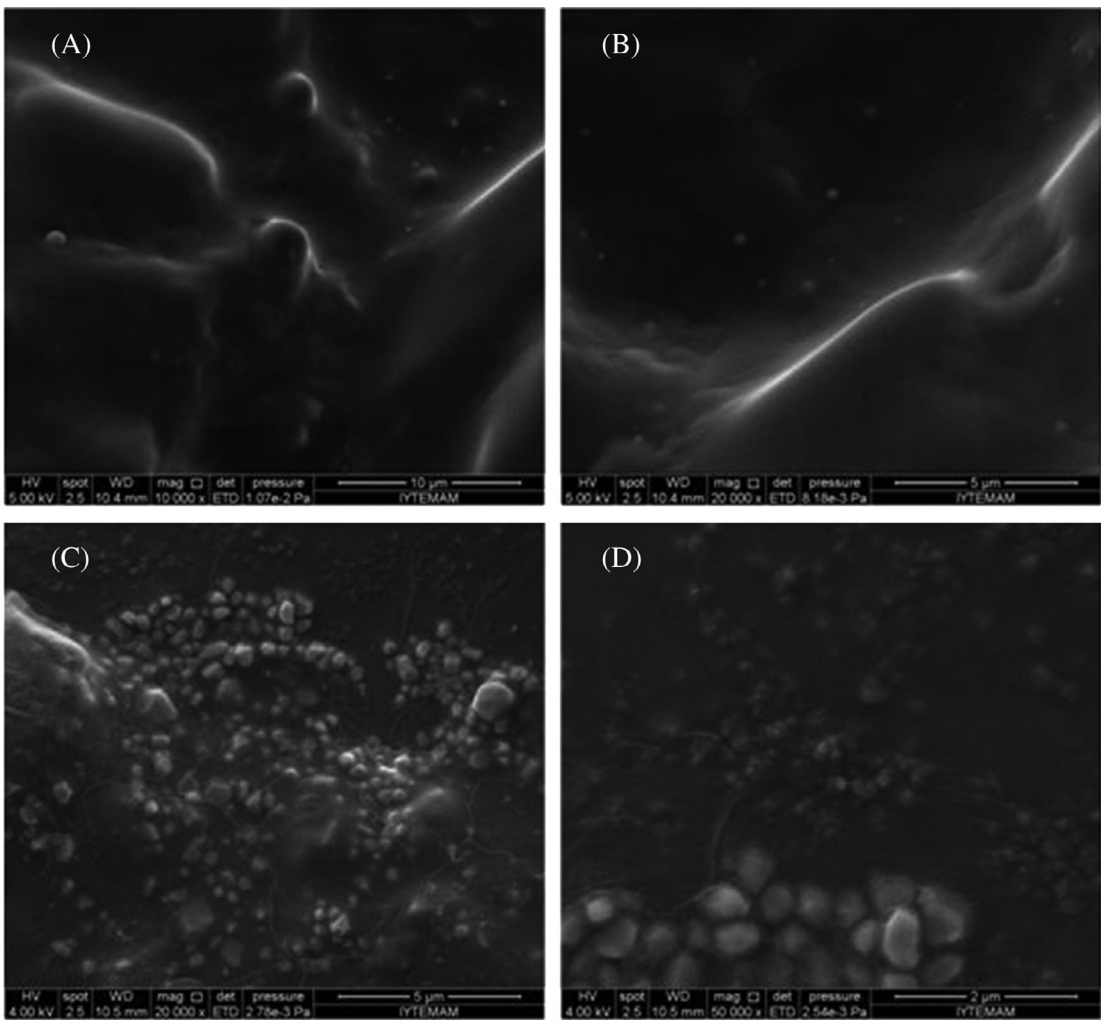

Figure 3. Empty niosome vesicles at 10.000× (A), 20.000× magnifications (B), propolis extract loaded niosomes at 20.000× (C) and 50.000× magnifications (D).

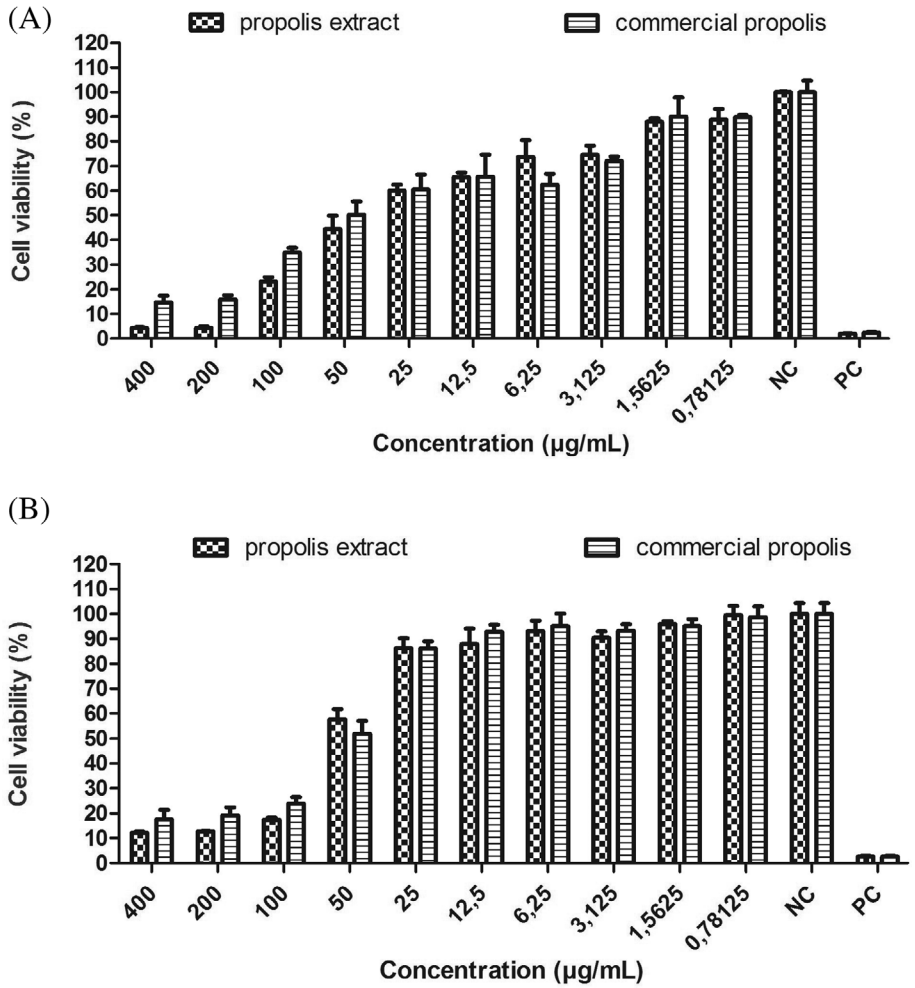

Figure 4. Dose-dependent cytotoxic effects of propolis extract and commercial propolis on A549 lung cancer cells (A) and BEAS-2B healthy lung cells (B) after 72 h exposure.

the cell viabilities were above 80% for 7 days for both cells (Fig. 5 (A), (C)). A significant cytotoxic effect of propolis on lung cancer cells in comparison to the lung epithelial cells (Fig. 5(A), (C)) was found by a two-way ANOVA with Bonferroni post-tests ($P < 0.001$ for 24 h, $P < 0.05$ for 72 and 168 h). A 3D system was designed by non-adhesive molds and cytotoxicities of empty and propolis-loaded niosomes were assessed on A549 and BEAS-2B cell spheroids by live/dead fluorescent dying test for 7 days. Spheroids of A549 cells were successfully formed on agar 3D micro tissue molds at the end of 10 days (Fig. 6(A)), reaching an average diameter of about 313 ± 11.6 µm. However, BEAS-2B healthy lung epithelial cells (wild type) did not form spheroids at the end of 10 days in our study (Fig. 6(B)). For this reason, the cytotoxicity test of propolis-loaded niosomes in BEAS-2B cells in 3D culture could not be performed. It was observed that A549 lung-cancer cells proliferated with high viability and formed a fully spheroid structure by filling the wells on the mold after 10 days, exhibiting tumor-formation efficiency.

After the formation of spheroids with A549 cells was observed, the spheroids were treated with propolis-loaded and empty niosomes. Although a significant change was not observed in average spheroid dimensions, there was a very slight loss of cell viability (decreasing green color) in spheroids and a significant increase in cell scattering (separation of cells from spheroids) with live ($P < 0.001$) and dead cells ($P < 0.05$ for day 0 versus day 3, $P < 0.001$ for day 0 versus day 7) from the spheroid structures in the untreated control group depending on the time when they were analyzed with ImageJ. This was shown by a two-way ANOVA with Bonferroni post-tests (Fig. 6(C), (F)). The decrease in cell viability is represented by the decreased green color and increased red color. The amount of cell scattering from the spheroids also showed an increase in cytotoxicity. So, propolis-loaded niosomes had increased cytotoxicity compared to the empty niosomes (Fig. 6(D), (E)). When scattered dead cells were examined, empty niosomes were no more toxic than the control group ($P > 0.05$), whereas a significant increase ($P < 0.001$) in scattered dead cells was noted subsequent to propolis-loaded niosome treatment on day 7 (one-way ANOVA with a Bonferroni multiple comparison test) (Fig. 6(G)).

DISCUSSION

Niosomes consist of lamellar structures that are formed by a mixture of non-ionic surfactants as the bilayer component and cholesterol as the membrane-stabilizing agent.[25] The particle size of propolis-loaded niosomes was 151 ± 2.84 nm with a zeta potential of −30.9 ± 0.33 mV. In a previous study, propolis-loaded niosomes were reported to have vesicle sizes between 294 and

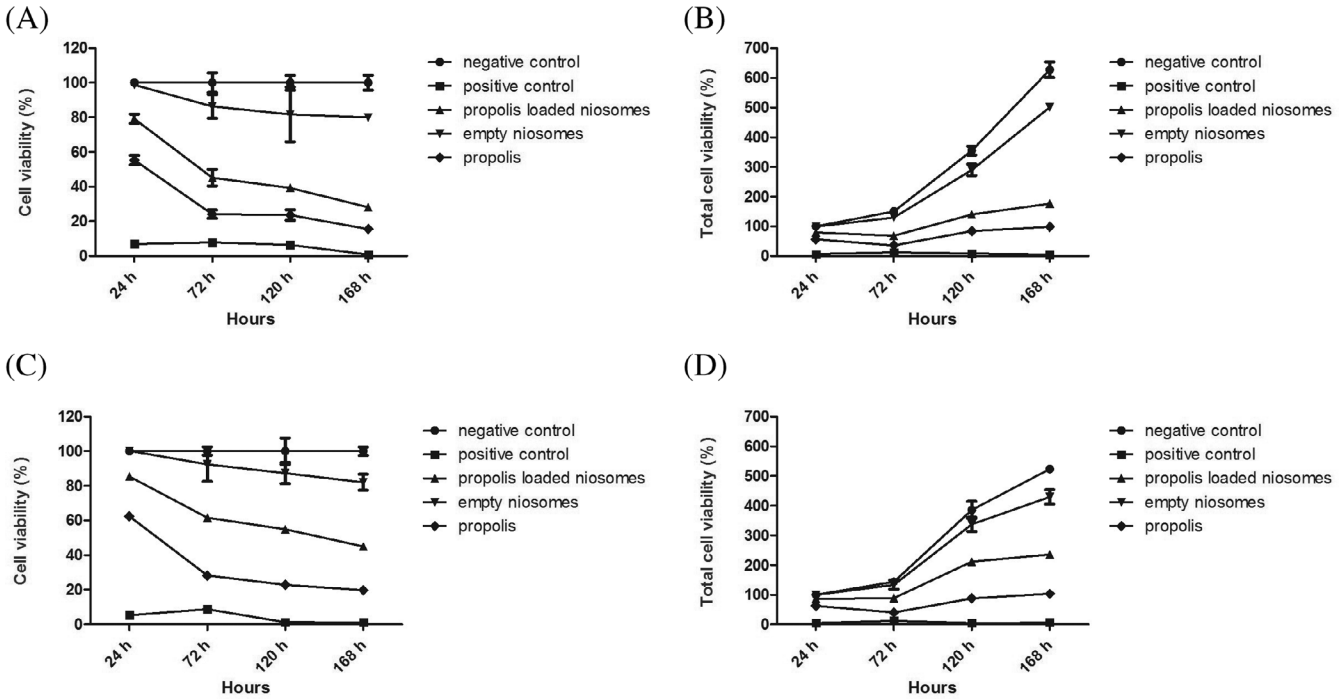

Figure 5. Two-dimensional cytotoxic effect of propolis-loaded niosomes, equivalent amount of free propolis, and empty niosomes on A549 lung cancer cells (A, B) and BEAS-2B healthy lung cells (C, D) for 7 days.

427 nm, and entrapment in the range of 50.62–71.29%,[26] where 71.29% efficiency was achieved with a particle size of 427 nm, which is 2.8 times larger than the loaded niosomes in our study.[27]

A similar zeta potential value of −30.67 ± 0.45 mV was also reported in a previous study where diallyl disulfide compound was encapsulated in Span 80 niosomes.[3] The zeta potential of niosomes plays an important role in storage and administration. The zeta potentials were measured as −18.6 ± 0.59 and − 30.9 ± 0.33 mV for empty and propolis-loaded niosomes, respectively. The surface charge of niosomes increased when loaded with the propolis extract. As the zeta potential charges increase, the charged particles repel one another, meaning that charged niosomes are more stable against aggregation and fusion than uncharged vesicles.[28] Regarding drug entrapment, the major compound was identified as galangin, which agreed well with a previous study,[29] and galangin-rich propolis extract was loaded with an encapsulation efficiency of 70%.

Free propolis extract showed a slight increase in dose-dependent cytotoxicity against A549 lung-cancer cells with an IC_{50} value of 25.44 ± 4.97 μg mL^{-1} for 72 h compared with commercial propolis (30.65 ± 7.43 μg mL^{-1}), which is from unknown sources. Similarly, the IC_{50} value of propolis originating from Turkey was reported as 31.7 ± 0.26 μg mL^{-1} on A549 cells and 76.9 ± 2.9 μg mL^{-1} on human normal foreskin fibroblast cells after 72 h,[7] which is in accordance with our results. Many research studies report that the biological properties of propolis are related to its chemical composition, which could vary based on geographical location, the genetic variability of the queen bee, the technique used for production, and the season in which propolis was collected.[12,30] It is therefore common for the biological activity and cytotoxic effects of propolis to differ. Indeed, the IC_{50} value of Brazilian green propolis was reported as 69.17 ± 11.28 μg L^{-1} for A549 cells, but with an almost twofold higher value (>100 μg L^{-1}) for Vero (African green monkey kidney epithelial cell line) cells.[6] The differences in cytotoxicity results might be associated not only with the natural sources of propolis extracts but also with the organism (human, monkey, mouse, etc.) and tissue type (lung, skin, kidney, etc.) in which the cells were used in cytotoxicity tests, and their metabolic activities and culture conditions.[31,32]

In some other studies, galangin (3,5,7-trihydroxyflavone) has been tested individually against various cancer cell lines such as human osteosarcoma (IC_{50}: 63.45 μg mL^{-1}),[33] murine melanoma cells (39.18 μg mL^{-1}),[34] and gastric cancer cells (27.02 μg mL^{-1}).[35] The results of one of these studies revealed the antimetastatic activity of galangin, which inhibited the formation of tumor colonies in the lung tissue in a C57BL/6J mouse lung metastatic model using B16F10 melanoma cells. Inhibition of melanoma metastasis was associated with decreased focal adhesion kinase expression based on immunochemical analyses.[36] So, it was thought that the cytotoxic activity of propolis extract originated from its galangin-rich composition.

Despite the broad therapeutic potential of propolis, its low solubility and physical instability present major hurdles with regard to its processing and formulation development. On the other hand, niosomes could encapsulate both hydrophilic and hydrophobic drug moieties and also reduce toxicity, enhance bioavailability, and sustain the release of the drug molecules.[23] Newly synthesized propolis-loaded niosomes decreased cell viability to a level below 30%, whereas empty niosomes proved to be non-cytotoxic because the cell viabilities were above 80% at the end of 7 days in a 2D setting, which is in agreement with a previous study[37] of the cytotoxicity of niosomes synthesized with Span60 and cholesterol against human melanoma A-375 and human keratinocyte HaCaT cells.

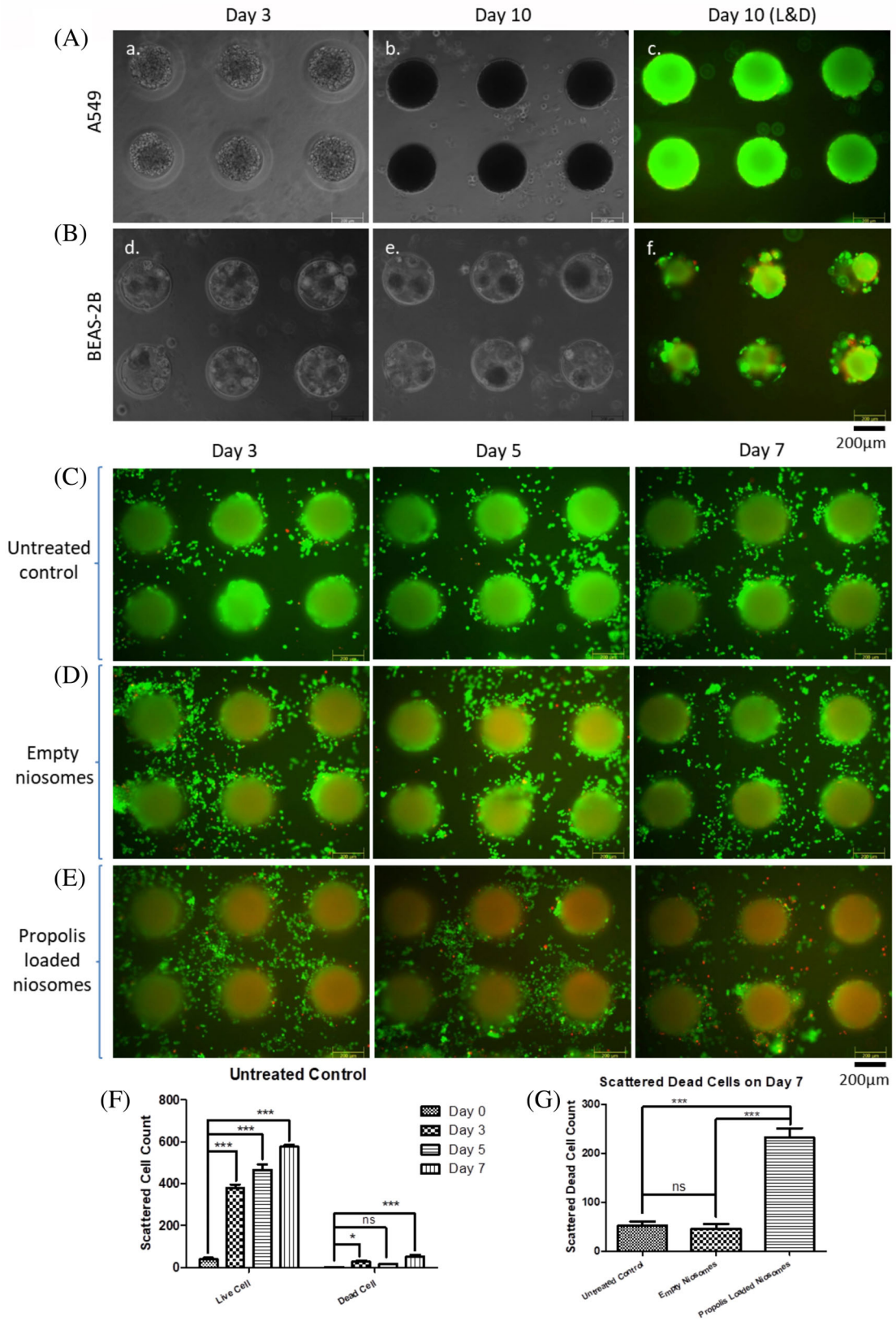

Figure 6. The light microscope images of A549 cells on day 3 and day 10 (a, b), live/dead fluorescent microscope image on day 10 (c) (A); the light microscope images of BEAS-2B healthy lung cells on day 3 and day 10 (d, e), live/dead fluorescent microscope image on day 10 (f) on 3D agar micro tissue mold (B); the fluorescent microscope images of untreated control group (C); empty niosomes (D); propolis-loaded niosomes (E) on A549 lung cancer cell spheroids on 3D agar micro tissue mold after live/dead assay on day 3, day 5 and day 7 (Zeiss, 10X, bar scale at 200 µm); scattered live/dead cell count of untreated A549 lung cancer cell spheroids day to day (two-way ANOVA with Bonferroni post-tests) (F); scattered dead cell count of untreated control group compared to propolis-loaded niosomes and empty niosomes on day 7 (one-way ANOVA Bonferroni multiple comparison test) (G) (ns: non-significant, *: $P < 0.05$, ***:$P < 0.001$).

Because of the inability of 2D cell culture to mimic the *in vivo* pathophysiology and microenvironment, we developed A549 spheroids as the 3D system using non-adhesive micro tissue molds. Spheroids of A549 cells reached a diameter of 313 ± 11.6 μm at the end of 10 days, providing a proper support, whereas BEAS-2B healthy lung epithelial cells (wild type) did not form spheroids. In a recent study, A549 3D spheroids cultured in the fabricated lab-on-a-chip system were reported to reach an average diameter of 500 μm over a 10-day culture.[38] Moreover, it was shown that the sphere formation of wild type BEAS-2B was not achieved, whereas BEAS-2B CD164 cells formed spheres reaching 200–300 μm in diameter after 10–14 days in sultralow plate.[39] In our study, when the propolis-loaded niosomes were administered to A549 3D spheroids, dead-cell scattering was five-fold higher than with untreated cells, whereas empty niosomes were not toxic to A549 spheroids.

In conclusion, both free propolis extract and propolis-loaded niosomes synthesized by the ether injection method with the mean size of 151 nm and − 30.9 mV zeta potential were shown to exhibit high cytotoxicity against lung-cancer cells in comparison to lung epithelial cells. Free propolis is more cytotoxic than propolis-loaded niosomes towards both A549 and BEAS-2B cells. This is probably due to the fact that the total amount of propolis released to the cells within a given time can be tolerated based on the diffusion rates and cellular uptake. Thus, propolis released from niosomes exhibited toxicity to tumor spheroids formed by A549 cells in a 3D setting, suggesting that they can be used as an effective nano-vesicle.

ACKNOWLEDGEMENTS

Access to the facilities of Natural Product Chemistry Laboratory at Bioengineering Department and FABAL Laboratory at the Faculty of Pharmacy at Ege University are appreciated.

AUTHOR CONTRIBUTIONS

Ozlem Yesil-Celiktas (O.Y.C.), Fulden Ulucan (F.U.), Esra Ilhan-Ayisigi (E.I.A.), and Ecem Saygili (E.S.) designed the study and the experiments. F.U., E.I.A., E.S. and Pelin Saglam-Metiner (P.S.M.) performed the experiments; Sultan Gulce-Iz (S.G.I.) and O.Y.C. supervised the cell culture aspects of the study. F.U., E.I.A., E.S., P.S.M., and O.Y.C. wrote the paper. O.Y.C. supervised the research and edited the manuscript. All authors read and approved the final manuscript.

REFERENCES

1 Wagner ME and Rizvi SSH, Novel method of niosome generation using supercritical carbon dioxide part I : process mechanics. *J Liposome Res* **25**:334–346 (2016).
2 Tian M, Han J, Ye A, Liu W and Xu X, Structural characterization and biological fate of lactoferrin-loaded liposomes during simulated infant digestion running title: in vitro infant digestion behavior of lactoferrin-loaded liposomes. *J Sci Food Agric* **99**:2677–2684 (2019).
3 Alam M, Zubair S, Farazuddin M, Ahmad E, Khan A, Zia Q *et al.*, Development, characterization and efficacy of niosomal diallyl disulfide in treatment of disseminated murine candidiasis. *Nanomedicine* **9**: 247–256 (2013).
4 Xu Y, Chen W, Tsosie J, Xie X, Li P, Wan J *et al.*, Niosome encapsulation of Curcumin: characterization and cytotoxic effect on ovarian cancer cells. *J Nanomater* **2016**:6365295 (2016).
5 Hayakari R, Matsumiya T, Xing F, Tayone JC, Dempoya J, Tatsuta T *et al.*, Effects of Brazilian green propolis on double-stranded RNA-mediated induction of interferon-inducible gene and inhibition of recruitment of polymorphonuclear cells. *J Sci Food Agric* **93**: 646–651 (2012).
6 Friõn-Herrera Y, Diaz-Garcia A, Ruiz-Fuentez J, Rodriguez-Sanchez H and Sforcin JM, Brazilian green propolis induced apoptosis in human lung cancer A549 cells through mitochondrial-mediated pathway. *J Pharm Pharmacol* **67**:1448–1456 (2015).
7 Demir S, Aliyazicioglu Y, Turan I, Misirli S, Mentese A, Yaman SO *et al.*, Antiproliferative and proapoptotic activity of Turkish propolis on human lung cancer cell line. *Nutr Cancer* **68**:165–172 (2016).
8 Uzel A, Sorkun K, Önçağ Ö, Çoğulu D, Gençay Ö and Salih B, Chemical compositions and antimicrobial activities of four different Anatolian propolis samples. *Microbiol Res* **160**:189–195 (2005).
9 Al-ani I, Zimmermann S, Reichling J and Wink M, Antimicrobial activities of European Propolis collected from various geographic origins alone and in combination with antibiotics. *Medicines* **5**: 1–17 (2018).
10 Kuropatnicki AK, Szliszka E and Krol W, Historical aspects of propolis research in modern times historical aspects of propolis research in modern times. *Evid Based Complement Alternat Med* **2013**:964149 (2013). https://doi.org/10.1155/2013/964149.
11 Curti V, Zaccaria V, Jorel A, Sokeng T, Dacrema M, Masiello I *et al.*, Bioavailability and in vivo antioxidant activity of a standardized polyphenol mixture extracted from Brown Propolis. *Int J Mol Sci* **20**: 1250 (2019).
12 do Nascimento TG, da Silva PF, Azevedo LF, da Rocha LG, de Moraes Porto IC, Lima TF *et al.*, Polymeric nanoparticles of Brazilian red propolis extract: preparation, characterization, antioxidant and leishmanicidal activity. *Nanoscale Res Lett* **11**:301 (2016).
13 Saglam-Metiner P, Gulce-Iz S and Biray-Avci C, Bioengineering-inspired three dimensional culture systems: Organoids to create tumor microenvironment. *Gene* **686**:203–212 (2019).
14 Ozdemir E, Sendemir-Urkmez A and Yesil-Celiktas O, Supercritical CO2 processing of a chitosan-based scaffold: can implantation of osteoblastic cells be enhanced? *J Supercrit Fluids* **75**:120–127 (2013).
15 Yildiz-Ozturk E, Gulce-Iz S, Anil M and Yesil-Celiktas O, Cytotoxic responses of carnosic acid and doxorubicin on breast cancer cells doped in butterfly-shaped microchips in comparison to 2D and 3D culture systems. *Cytotechnology* **69**:337–347 (2017).
16 Onbas R, Kazan A, Nalbantsoy A and Yesil-Celiktas O, Cytotoxic and nitric oxide inhibition activities of Propolis extract along with microencapsulation by complex Coacervation. *Plant Foods Hum Nutr* **71**: 286–293 (2016).
17 Parthibarajan R, Pradeep Kumar S, Gowri SN, Balakishan L, Srinivas B, Bhagya Laxmı V *et al.*, Design and in vitro evaluation of voriconazole niosomes. *Int J Pharm Pharm Sci* **5**:604–611 (2013).
18 Verza S, Pavei C, Borré GL, Silva APC, Ortega GG and Mayorga P, Determination of galangin in commercial extracts of *Alpinia officinarum* by RP-HLPC-DAD. *Lat Am J Pharm* **30**:576–579 (2011).
19 Zu Y, Zhang Y, Wang W, Zhao X, Han X, Wang K *et al.*, Preparation and in vitro/in vivo evaluation of resveratrol-loaded carboxymethyl chitosan nanoparticles. *Drug Deliv* **23**:971–981 (2014).
20 Desroches BR, Zhang P, Choi BR, King ME, Maldonado AE, Li W *et al.*, Functional scaffold-free 3-D cardiac microtissues: a novel model for the investigation of heart cells. *Am J Physiol Heart Circ Physiol* **302**:2031–2042 (2012).
21 Kasote DM, Pawar MV, Bhatia RS, Nandre VS, Gundu SS, Jagtap SD *et al.*, HPLC, NMR based chemical profiling and biological characterisation of Indian propolis. *Fitoterapia* **122**:52–60 (2017).
22 Oliveira RN, Mancini MC, Cabral F, De Oliveira S, Passos TM, Quilty B *et al.*, FTIR analysis and quantification of phenols and flavonoids of five commercially available plants extracts used in wound healing. *Rev Mater* **21**:767–779 (2016).
23 Khan MI, Madni MA, Ahmad S, Mahmood MA, Rehman M and Asfaq M, Formulation design and characterization of a non-ionic surfactant based vesicular system for the sustained delivery of a new chondroprotective agent. *Braz J Pharm Sci* **51**:607–615 (2015).
24 Dong L-L, Zhang C-F, Zhang Y-Y, Bai Y-X, Jin G, Suna Y-P *et al.*, Improving CO2/N2 separation performance using nonionic surfactant tween containing polymeric gel membranes. *RSC Adv* **5**:4947–4957 (2015).
25 Barani M, Nematollahib MH, Maryam Z, Mirzaeia M, Torkzadeh-Mahanid M, Pardakhtye A *et al.*, In silico and in vitro study of magnetic niosomes for gene delivery: the effect of ergosterol and cholesterol. *Mater Sci Eng C* **94**:234–246 (2019).
26 Patel J, Ketkar S, Patil S, Fearnley J, Mahadik KR and Paradkar AR, Potentiating antimicrobial efficacy of propolis through niosomal-based system for administration. *Integr Med Res* **4**:94–101 (2015).

27 Ali M, Motaal AA, Ahmed MA, Alsayari A and El-Gazayerly ON, An in vivo study of *Hypericum perforatum* in a niosomal topical drug delivery system. *Drug Deliv* **25**:417–425 (2018).
28 Moghassemi S and Hadjizadeh A, Nano-niosomes as nanoscale drug delivery systems: an illustrated review. *J Control Release* **185**:22–36 (2014).
29 Bertelli D, Papotti G, Bortolotti L, Marcazzan GL and Plessi M, 1H-NMR simultaneous identification of health-relevant compounds in Propolis extracts. *Phytochem Anal* **23**:260–266 (2012).
30 Toreti VC, Sato HH, Pastore GM and Park YK, Recent Progress of Propolis for its biological and chemical compositions and its botanical origin. *Evid Based Complement Alternat Med* **3**:697390 (2013).
31 Butler M, *Animal Cell Culture and Technology*, 2nd edn. BIOS Scientific Publishers, NewYork (2004).
32 Freshney RI, *Culture of Animal Cells: A Manual of Basic Technique*, 5th edn. John Wiley & Sons, Hoboken, NJ (2005).
33 Yang Z, Li X, Han W, Lu X, Jin S, Yang W *et al.*, Galangin suppresses human osteosarcoma cells: an exploration of its underlying mechanism. *Oncol Rep* **37**:435–441 (2017).
34 Zhang W, Lan Y, Huang Q and Hua Z, Galangin induces B16F10 melanoma cell apoptosis via mitochondrial pathway and sustained activation of p38 MAPK. *Cytotechnology* **65**:447–455 (2013).
35 Kim D, Jeon YK and Nam MJ, Galangin induces apoptosis in gastric cancer cells via regulation of ubiquitin carboxy-terminal hydrolase isozyme L1 and glutathione Stransferase P. *Food Chem Toxicol* **50**: 684–688 (2012).
36 Zhang B, Tang Q, Huang Z and Hua W, Galangin inhibits tumor growth and metastasis of B16F10 melanoma. *J Cell Biochem* **114**:152–161 (2013).
37 Dwivedi A, Mazumder A, du Plessis L, du Preez JL, Haynes RK and du Plessis J, In vitro anti-cancer effects of artemisone nano-vesicular formulations on melanoma cells. *Nanomedicine* **11**:2041–2050 (2015).
38 Zuchowska A, Jastrzebska E, Chudy M, Dybko A and Brzozka Z, 3D lung spheroid cultures for evaluation of photodynamic therapy (PDT) procedures in microfluidic lab-on-a-Chip system. *Anal Chim Acta* **990**:110–120 (2017).
39 Chen WL, Huang AF, Huang SM, Ho CL, Chang YL and Chan JY, CD164 promotes lung tumor-initiating cells with stem cell activity and determines tumor growth and drug resistance via Akt/mTOR signalling. *Oncotarget* **8**:54115–54135 (2017).

